Assembly and Suppression of Endogenous Kv1.3 Channels in Human T Cells

GYÖRGY PANYI*‡ and CAROL DEUTSCH*

*Department of Physiology, University of Pennsylvania, Philadelphia, Pennsylvania 19104-6085; and ‡Department of Biophysics, University Medical School of Debrecen, Debrecen, 4012 Hungary

ABSTRACT The predominant K^+ channel in human T lymphocytes is Kv1.3, which inactivates by a C-type mechanism. To study assembly of these tetrameric channels in Jurkat, a human T-lymphocyte cell line, we have characterized the formation of heterotetrameric channels between endogenous wild-type (WT) Kv1.3 subunits and heterologously expressed mutant (A413V) Kv1.3 subunits. We use a kinetic analysis of C-type inactivation of currents produced by homotetrameric channels and heterotetrameric channels to determine the distribution of channels with different subunit stoichiometries. The distributions are well-described by either a binomial distribution or a binomial distribution plus a fraction of WT homotetramers, indicating that subunit assembly is a random process and that tetramers expressed in the plasma membrane do not dissociate and reassemble. Additionally, endogenous Kv1.3 current is suppressed by a heterologously expressed truncated Kv1.3 that contains the amino terminus and the first two transmembrane segments. The time course for suppression, which is maximal at 48 h after transfection, overlaps with the time interval for heterotetramer formation between heterologously expressed A413V and endogenous WT channels. Our findings suggest that diversity of K^+ channel subtypes in a cell is regulated not by spatial segregation of monomeric pools, but rather by the degree of temporal overlap and the kinetics of subunit expression.

INTRODUCTION

Human T lymphocytes contain voltage-gated K^+ channels (400–750 channels/cell [Cahalan et al., 1985; Deutsch et al., 1986; Deutsch et al., 1991]). These channels, composed of four identical subunits (MacKinnon, 1991), are encoded by the Kv1.3 gene (Cai et al., 1992) and determine the resting membrane potential in human T cells (Leonard et al., 1992). At its resting potential of −70 mV (Deutsch et al., 1979; Rink et al., 1980; Gelfand et al., 1984), the T cell has an extremely high input impedance, ~20 Gohms, and thus opening of only one K^+ channel is sufficient to drive the membrane toward more negative membrane potentials (Lee et al., 1992). At least two important functions in the T cell depend on membrane potential. First, volume regulation in response to hypotonic shock is determined by electrochemical driving forces (Grinstein and Smith, 1990; Deutsch and Chen, 1993), and second, mitogenic interleukin-2 production and proliferation is sensitive to membrane potential, thus implicating a role for Kv1.3 in mitogenesis (Bono et al., 1989; Freedman et al., 1992; Lin et al., 1993). Therefore it is important to understand what governs not only the biophysical properties of these channels but also the formation of functional K^+ channels. The density of K^+ channels at the surface of the cell depends on transcriptional and translational regulation of subunits, their association to form tetramers, and the integration of these tetramers into the plasma membrane. How and where Kv1.3 subunits assemble is not known, nor whether these tetrameric channels in the plasma membrane are in equilibrium with monomeric pools of subunits. For most plasma membrane proteins multimerization occurs posttranslationally in the endoplasmic reticulum (ER) and is often a prerequisite for efficient export of these proteins from the ER (Doms et al., 1993; Hurtley and Helenius, 1989). Proper folding of protein subunits produces the required topology for specific quaternary contacts allowing multimerization between appropriate assembly partners. The time for assembly of different proteins ranges from minutes to hours after synthesis (Carlin and Merlie, 1986). Although the ER is the primary site of multimerization, other compartments later in the secretory pathway can host further assembly reactions (Rotundo, 1984; Sporn et al., 1986).

Address correspondence to Dr. Carol Deutsch, Department of Physiology, University of Pennsylvania, 3700 Hamilton Walk, Richards Bldg. D-203, Philadelphia, PA 19104-6085.

J. GEN. PHYSIOL. © The Rockefeller University Press • 0022-1295/96/03/409/12 $2.00
Volume 107 March 1996 409–420

Compared to other membrane proteins (e.g., receptors, ectoenzymes, viral antigens, MHC antigens, Na^+,K^+-ATPases) and secretory and lysosomal proteins (e.g., immunoglobulins, glycoprotein hormones, extracellular matrix components), assembly of voltage-gated ion channels in general, and K^+ channels, in particular, has not been well-characterized. (However, see Li et al., 1992; Shen et al., 1993; Babila et al., 1994; Hopkins et al., 1994; Lee et al., 1994; Santacruz-Toloza et al., 1994; Shen and Pfaffinger, 1995; Tu et al., 1995). To determine (*a*) whether endogenous subunits can assemble with heterologously transfected subunits, (*b*) whether tetrameric channels in the plasma membrane ever dissociate, and (*c*) whether assembly of endogenous channels can be suppressed by truncated Kv1.3 peptides, we have analyzed mixed K^+ channel tetramers that are functionally distinguishable. We have previously used this approach to show that all four subunits of the tetrameric Kv1.3 participate cooperatively in C-type inactivation (Panyi et al., 1995). In these experiments, wild-type and mutant Kv1.3 homo- and heterotetrameric currents, each manifesting markedly different and identifiable inactivation kinetics, were produced heterologously in a murine lymphoid expression system. A kinetic analysis of these currents permitted channel subunit composition and its consequences for channel gating to be determined. In this paper, we use a similar strategy in Jurkat cells, a human T cell leukemia line that expresses endogenous Kv1.3 (Decoursey et al., 1985), to study K^+-channel assembly.

MATERIALS AND METHODS

Transfection of Jurkat Cells

Jurkat cells, transformed with SV-40 large T antigen (TagC15; Northrop et al., 1993), were cultured at $<1 \times 10^6$/ml and passaged every 2–3 d. Twenty-four hours before transfection, cells were transferred to fresh media, and collected in the logarithmic phase of growth. Cells were suspended in Hank's-20 mM HEPES balanced salt solution +10% FBS (pH = 7.23) at 1.4×10^7 cells/ml, and the appropriate plasmid DNA was added to the cell suspension (see below). The cell suspension was transferred to electroporation cuvettes (400 μl/cuvette, 4-mm electrode gap), kept on ice for 10 min, and then electroporated using a BTX-electroporator (San Diego, CA) with settings previously determined to give ~50% viability at 24 h after transfection (875 V/cm, 2200 μF, 13Ω). The resultant time constants were 24–25 ms. Cells were incubated for an additional 10 min on ice, transferred back to culture medium at $\sim 0.5 \times 10^6$ cells/ml, and cultured for 6–72 h at 37°C, 5% CO_2.

For transient transfection of cells with Kv1.3(A413V), a double-gene plasmid encoding the mutant K^+ channel and a membrane surface molecule, human CD20, (pRc/CMV/A413V/CD20, 8.7 kb) was added to the cell suspension in different concentrations (8–25 nM) before electroporation. Construction of the double-gene plasmid and the mutation of alanine to valine at position 413 was described by Panyi et al. (1995).

For suppression experiments, a double-gene plasmid encoding a truncated K^+ channel (only the first 866 NH_2-terminal bases of Kv1.3 corresponding to the NH_2 terminus and the first two transmembrane segments of the channel protein) and a membrane surface molecule, mouse CD4 (pRc/CMV/Kv1.3(+866)/mCD4, 8.8 kb), were added (25 nM) to the cell suspension before electroporation. Construction of the double-gene plasmid and the deletion mutation of Kv1.3 has been described in Tu et al. (1995). Control cells for these experiments were transfected with 25 nM of pRc/CMV/mCD4 (6.8 kb; Tu et al., 1995). Transfection of, and current recording from, control samples were shifted 3 h later than experimental samples to ensure that cells were cultured for equal periods of time between transfection and current recording.

Electrophysiology

Jurkat cells were collected from culture and incubated for 30 min on ice with phosphate buffered saline (PBS) supplemented with 5% fetal bovine serum, which also contained 2% rabbit serum and 2% goat serum to block nonspecific F_c receptor binding of the antibodies used for selectively adhering the transfected cells. Cells expressing human CD20 or mCD4 were adhered to 35-mm petri dishes coated with monoclonal mouse anti–human CD20 antibody (Immunotech, Westbrook, ME) or monoclonal rat anti–mouse CD4 (PharMingen, San Diego, CA), respectively, for 45 min at room temperature as described previously (Matteson and Deutsch, 1984; Deutsch and Chen, 1993). Dishes were washed gently seven times with 1 ml of PBS and twice with 1 ml of normal extracellular bath medium (see below). Standard whole-cell patch-clamp techniques were used, as described previously (Matteson and Deutsch, 1984). Pipettes were made from SG10 glass (Richland Glass Co., Richland, NJ), coated with Sylgard 184 (Dow Corning, Midland, MI), and fire-polished to give electrodes of 2–3.3 MΩ resistance in the bath. The bath solution was (in mM): 145 NaCl, 5 KCl, 1 $MgCl_2$, 2.5 $CaCl_2$, 5.5 glucose, 10 HEPES, (pH 7.35, 305 mOsm). The pipette solution was (in mM): 130 KF, 11 K_2EGTA, 1 $CaCl_2$, 2 $MgCl_2$, and 10 HEPES (pH 7.20, 282 mOsm). Because of the large amplitude of K^+ currents in transfected cells, we used up to 85% compensation of the series resistance. Holding potential was −120 mV. Current recordings were started 2–5 min after achieving the whole-cell configuration and continued for 12–15 min. In most cases the characteristics of the K^+ current were stable during this recording period. All experiments were carried out at room temperature.

Data Analysis

Before analysis, current traces were corrected for ohmic leak and for voltage error caused by series resistance (program by D. Levy and G. Panyi) according to Panyi et al. (1995). Since both peak conductance and inactivation kinetics of Kv1.3 are voltage independent at membrane potentials >+20 mV, the corrected current traces for data obtained at +50 mV can be used to determine inactivation time constants. Voltage errors due to series resistance were typically < 8 mV.

The fraction of noninactivated channels (R, Eq. 1) was determined from the ratio of steady state to peak current after a depolarization to +50 mV. However, we had to correct for an average 13 pA leakage current in these Jurkat cells to account for the systematic tendency for large measured R values seen with

small peak currents (data not shown). After correcting R for this leakage current, there was no statistical difference (P = 0.06, Kruskal-Wallis ANOVA) in R values between WT homotetramers (median R was 0.029, n = 22), A413V homotetramers (median R was 0.016, n = 74), and mixtures of homo- and heterotetramers (median R was 0.024, n = 73).

Inactivation of K^+ currents at +50 mV was fit, as described in Results, according to the cooperative model in Panyi et al. (1995). The Marquardt-Levenberg algorithm was used to fit the appropriate equations to the decaying portion of the current traces. The fits were evaluated by the sum of squared differences between the measured and calculated data points [SSE = $\Sigma(y\text{-}\hat{y})^2$].

The distribution of the peak currents and the time constants were non-Gaussian ($P < 0.05$, Kolmogorov-Smirnov test) unless otherwise stated. Accordingly, the central tendency and dispersion of the data are reported as the median and the 25 and 75 percentile values, respectively, and the statistical comparisons were made using the appropriate nonparametric tests.

We classified transfected cells into three types, those expressing predominantly (*a*) homotetrameric wild-type (WT) Kv1.3, (*b*) homotetrameric A413V mutants, and (*c*) heterotetramers, using criteria based on the expected properties of the homotetramers. WT Kv1.3 currents in cells transfected only with mCD4 had inactivation time constants of 150.8 ± 36.3 ms (mean ± SD). We selected a lower boundary for the WT time constant of 96 ms, which is 1.5 × SD below the mean. This critical value is expected to include > 93% of cells expressing only WT channels. The upper range of inactivation time constant for currents produced by A413V mutant homotetrameric channels in Jurkat cells is 5.48 ms (see Results). A sum of two exponential terms were fit to the current traces

$$I(t) = A_f \times e^{-t/\tau_f} + A_s \times e^{-t/\tau_s} + C,$$

and the dominant time constant (i.e., the term containing the larger value of A) was compared to the lower and upper limits of WT and A413V inactivation time constants, respectively. A cell with a dominant inactivation time constant < 5.48 ms or > 96 ms was considered to express predominantly A413V or WT homotetramers, respectively. A dominant inactivation time constant between 5.48 ms and 96 ms was an indication that a cell expressed heterotetramers of WT and mutant subunits.

To evaluate the probability that a heterotetramer had a time constant outside of this range, we used a bootstrap method to estimate the distribution of the fastest and slowest time constants expected for heterotetramers (i.e., τ_3 and τ_1, see Results). This method is used to estimate the variance of a parameter derived from a nonparametric population (Efron and Tibshirani, 1984). As we show below, the distribution of inactivation time constants for A413V homotetramers is non-Gaussian. To estimate the expected range of heterotetrameric time constants from our measured data for homotetramers, we created a so-called bootstrap distribution. This distribution was obtained by random sampling with replacement of the inactivation time constants from cells expressing either homotetrameric A413V mutants or WT homotetramers, for each sampled pair of time constants and calculating τ_1 and τ_3 from Eq. 2. Repeating this procedure 1,000 times, we generated a bootstrap population of 1,000 pairs of τ_1 and τ_3. The probability of a heterotetramer having an inactivation time constant out of the 5.48–96-ms range for this population was $< 10^{-6}$.

RESULTS

Diversity of Currents Exhibited by Jurkat Cells Transfected with A413V Channel Gene

To determine whether endogenous WT Kv1.3 subunits can form heterotetrameric channels with heterologously expressed subunits, we have transfected Jurkat cells with a double-gene plasmid encoding both a mutant K^+ channel (Kv1.3(A413V)) and a membrane-surface protein, human CD20 (hCD20). Transfection with double-gene plasmids maximizes the cotransfection efficiency of antibody-selected cells (Tu et al., 1995). The Kv1.3(A413V) K^+ channel was chosen because the gating properties of this mutant permit functional tagging of mutant subunits in the presence of WT Kv1.3 (Panyi et al., 1995). Human CD20 was chosen as the cell surface marker because it is endogenously present only on human B cells, and therefore can be used in T cells regardless of species.

Kv1.3(A413V) expressed heterologously in CTLL-2, a mouse cytotoxic T cell line devoid of endogenous K^+ channels (Deutsch and Chen, 1993), produces current at +50 mV with very fast inactivation (inactivation time constant, τ_{inact} ~4 ms) compared to wild-type Kv1.3 (τ_{inact} ~200 ms). We have used this kinetic difference to determine the subunit composition of heterologously expressed channels derived from mixtures of WT and A413V Kv1.3 subunits in CTLL-2 (Panyi et al., 1995). We applied a similar analysis to establish whether heterotetrameric channels are formed in Jurkat cells between endogenous Kv1.3(WT) and heterologous Kv1.3 (A413V).

Whole-cell current elicited by a depolarization to +50 mV is shown in Fig. 1 for six Jurkat cells transfected with the double-gene plasmid. The time courses of inactivation for traces *a* and *b* were well-fit with a single-exponential function to give inactivation time constants (τ_{inact}) of 3.5 ms and 161.5 ms, and are characteristic of currents produced by homotetrameric A413V and WT channels, respectively (see below). Traces *c* and *d* show monophasic inactivation which, for illustrative purposes only, was estimated in each case by a single-exponential function to give inactivation time constants of 10.6 ms and 31 ms, respectively. Intermediate inactivation kinetics, as observed for cells *c* and *d*, are characteristic of currents carried by mixtures of homo- and heterotetrameric channels formed from A413V and WT Kv1.3 subunits (Panyi et al., 1995). By contrast, a mixture of two separate populations of homotetrameric WT and A413V channels with very different inactivation kinetics would produce a current decay characterized by biphasic kinetics and described by the sum of two exponential terms, each containing inactivation time constants characteristic for WT and A413V. Such an example is shown in *e*. Finally, *f* shows another type

of biphasic current that is qualitatively, but not quantitatively, similar to the trace in *e*. The slow phase of the decay is identical to that expected for pure WT current, but the fast component of the decay is slower than expected for a pure A413V current. Further analysis of this case is provided below. This wide variety of inactivation kinetics, illustrated in Fig. 1, *a–f*, reflects differences in DNA plasmid concentrations, efficiency of transcription and translation heterogeneity, times after the transfection, and different levels of endogenous WT channel expression (see below and Discussion).

Analysis of Heterotetrameric Currents

Using a statistical analysis of currents produced by a mixture of homo- and heterotetrameric Kv1.3 channels assembled from WT and A413V subunits in CTLL-2, we previously demonstrated that the mixture of channel types in the plasma membrane conforms to a binomial distribution (Panyi et al., 1995). Assuming a binomial distribution for the formation of heterotetrameric channels from WT and A413V subunits, the normalized current can be described by the following equation:

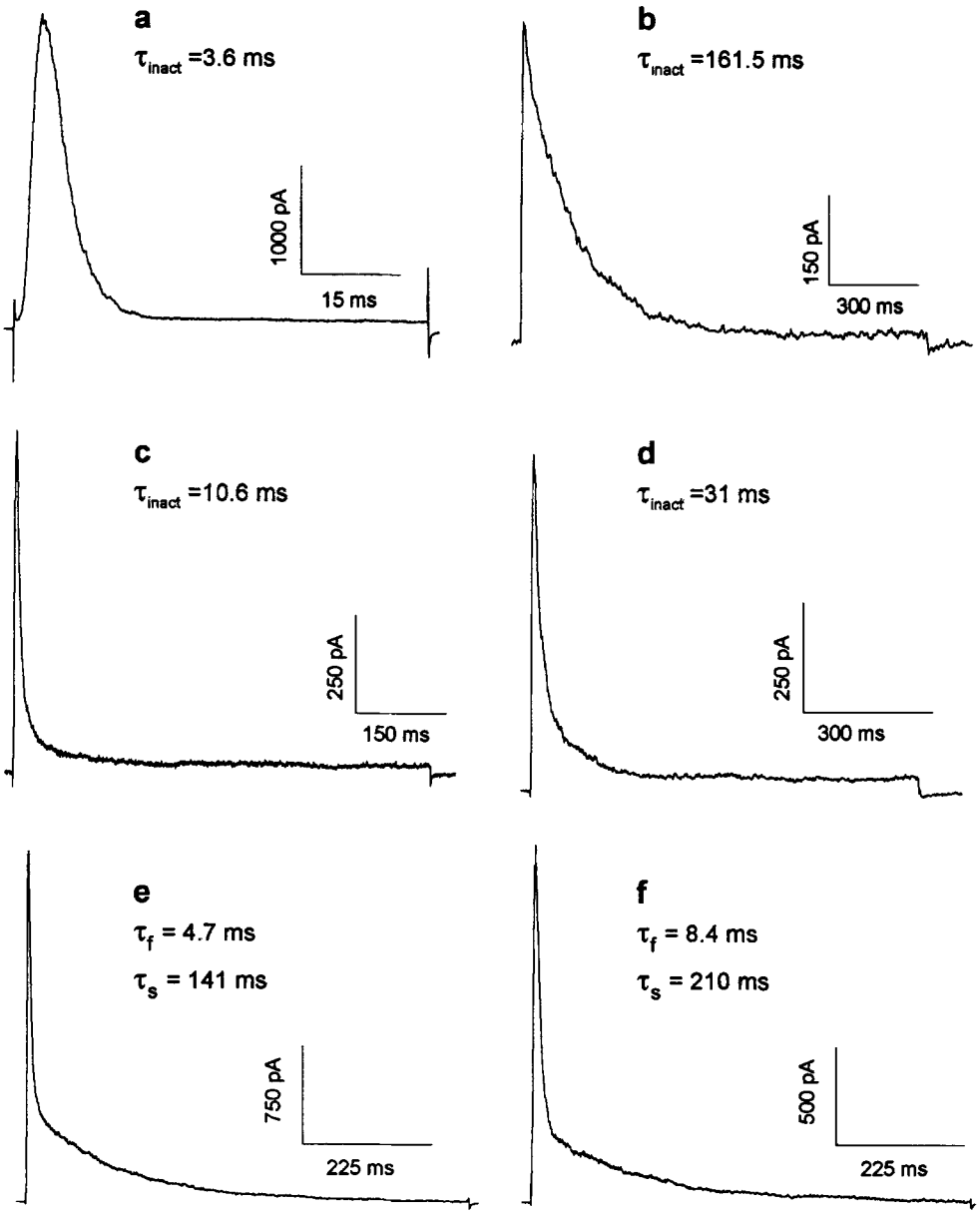

FIGURE 1. Whole-cell K^+ currents in Jurkat Tag C15 cells transfected with Kv1.3 (A413V). (*a–d*) Cells were transfected with Kv1.3 (A413V)/CD20 double-gene plasmid (25 nM). After 48–72 h currents were elicited by a voltage step from the holding potential of −120 to +50 mV. The current traces were corrected for ohmic leak and voltage error caused by series resistance as described in the Materials and Methods. The best fit single-exponential time constant (τ_{inact}) is indicated for each cell. Note difference in time and current scales. Sampling frequency, cell capacitance and series resistance were (*a*) 31.25 kHz, 3.1 pF, and 4.2 MΩ; (*b*) 666 Hz, 5.7 pF, and 10.2 MΩ; (*c*) 2.66 kHz, 10 pF, and 5.6 MΩ; and (*d*) 1 kHz, 12 pF, and 11 MΩ, respectively. (*e–f*) Cells were transfected with Kv1.3 (A413V)/CD20 double-gene plasmid (8 nM), and currents were recorded 6 h after the transfection as described for *a–d*. The sum of two exponential functions was fit to the current decays to give the fast (τ_f) and the slow (τ_s) components of the inactivation, which are displayed in the figure. Sampling frequency, cell capacitance and series resistance were (*e*) 3.9 kHz, 2.2 pF, and 7.5 MΩ; (*f*) 3.9 kHz, 3.2 pF, and 0.9 MΩ, respectively. *R* values were 0.027, 0.027, 0.015, 0.04, 0.004, and 0.004 for *a–f*, respectively.

$$\frac{I(t)}{I_{peak}} = \sum_{m=0}^{4} B_{4,m}\left((1-R)\,e^{-\frac{t}{\tau_m}} + R\right) \quad (1)$$

where $B_{4,m} = \frac{4!}{m!\,(4-m)!}p^m(1-p)^{4-m}$;

p is the estimated fraction of mutant subunits in the cell membrane; m indicates the number of mutant (A413V) subunits in a given channel; and R is the ratio of steady state current to peak current measured for each trace. The inactivation time constant characteristic for each heterotetramer (τ_m) can be calculated from experimentally determined τ_0 and τ_4, the inactivation time constants for WT and A413V homotetrameric currents, respectively, according to Panyi et al. (1995):

$$\tau_m = \frac{\tau_0}{F^m}, \text{ where } F = \sqrt[4]{\frac{\tau_0}{\tau_4}}. \quad (2)$$

Although we had previously determined τ_0 and τ_4 in CTLL-2 cells, it is possible that these time constants are different in Jurkat cells. Therefore, we determined τ_0 for endogenous Kv1.3 channels in Jurkat cells transfected with mCD4 (control) and τ_4 as described below. The distribution of τ_0 at +50 mV test potential was Gaussian ($P = 0.75$, Kolmogorov-Smirnov test) with a mean ± SD of 150.8 ± 36.3 ms ($n = 46$), and a median of 151.3 ms.

Since we cannot express A413V channels in Jurkat cells in isolation due to the presence of endogenous WT genes, we have determined τ_4 in cells where the level of the endogenous WT current was negligible as compared to the current carried by transfected A413V channels. The peak endogenous WT current at +50 mV in cells transfected with mCD4 (control) had small amplitudes with a median of 321 pA ($n = 84$, 25 percentile = 213 pA, 75 percentile = 525 pA). In cells transfected with A413V subunits we were able to record currents with at least an order of magnitude higher amplitude. To obviate the influence of heterotetramers on the determination of τ_4 we considered only those current traces where the peak current at +50 mV was > 5 nA. This limit is reasonable, since it is ~15 times higher than the median peak current produced by endogenous WT channels and approximately three times higher than the highest current amplitude (1747 pA at +50 mV) recorded from control (mCD4-transfected) cells. Out of 23 cells expressing currents > 5 nA, 20 showed current with single-exponential inactivation kinetics and three cells showed a biphasic current decay. These three current traces were each fit with a sum of two exponentials to resolve the fast (τ_f) and the slow (τ_s) components of decay, as described in the Materials and Methods. In all three cells the inactivation time constant for the slow component was greater than 96 ms, corresponding to WT current (see Materials and Methods section), and the ratio of the amplitude of the WT component to the fast component was < 0.05. The distribution of the time constants derived from either single-exponential fits (20 cells) or double-exponential fits (three cells, τ_f) had a median of 3.52 ms and a range from 2.56 ms to 5.48 ms. These results are in good agreement with our previous values obtained from pure homotetrameric A413V channels expressed in CTLL-2 cells, for which the median of the inactivation time constant was 4.02 ms (Panyi et al., 1995). We have compared the distribution of the time constants for pure homotetrameric A413V currents in CTLL-2 and Jurkat cells and found no significant difference in the median values ($P > 0.05$, Mann-Whitney U-test). Thus, these results indicate that the criterion used to determine τ_4 accurately identifies currents that are pure homotetrameric A413V.

Based on these results we set the upper limit of the inactivation time constants for homotetrameric A413V current to 5.48 ms, the slowest time constant that we found in cells expressing currents > 5 nA at +50 mV. We have tested the validity of this boundary condition experimentally as follows. Since the steady state inactivation of current carried by homotetrameric A413V channels is complete at −70 mV holding potential (G. Panyi and C. Deutsch, unpublished results), we have compared the current elicited by depolarizations to +50 mV from a holding potential (HP) of −120 mV to that elicited from a HP of −70 mV in seven cells expressing current with $\tau_f < 5.48$ ms. A representative experiment is shown in Fig. 2 *a*. Depolarization from a HP of −70 mV produces a current in which the fast inactivation rate completely disappears and the slow component remains unchanged. In all seven cells the fast component of the current decay at +50 mV vanished when the cell was held at −70 mV, indicating that this fast component was due primarily to homotetrameric A413V channels. Fig. 2 *b* shows that identical changes in the holding potential in a cell expressing only WT channels affects neither the current amplitude nor the inactivation kinetics.

Using Eq. 2 with $\tau_0 = 150.8$ ms and $\tau_4 = 3.52$ ms, we have calculated inactivation time constants $\tau_1 = 59$ ms, $\tau_2 = 23$ ms and $\tau_3 = 9$ ms, for channels containing 1, 2, and 3 mutant subunits, respectively. These values along with τ_0 and τ_4 were substituted into Eq. 1 and used to fit the decaying part of the normalized current traces shown in Fig. 3. The fitted parameter is p, the fraction of mutant subunits in the membrane. Fig. 3 shows that Eq. 1. gives good fits for some traces (i.e., *a* and *b*) but does not fit others (i.e., *c* and *d*), indicating that the binomial distribution does not always describe the distribution of channel subtypes. The cells in *a* and *b* differ in the calculated p values, i.e., for the cell shown in *a* the fraction of mutant subunits is 0.80 while for the cell

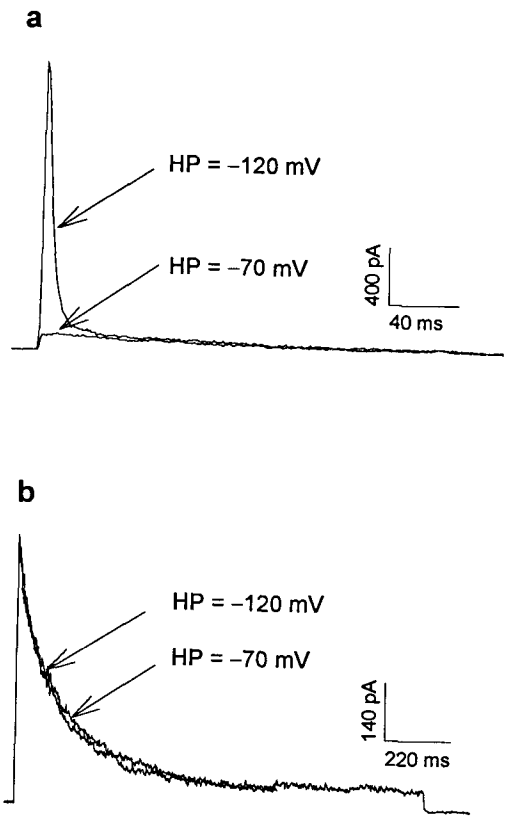

FIGURE 2. Separation of the fast and the slow component of the current by changing the holding potential. (*a–b*) Cells were transfected with Kv1.3(A413V)/CD20 double-gene plasmid (25 nM). After 24 (*a*) or 48 h (*b*) currents were recorded using whole-cell patch clamp, and traces were corrected for ohmic leak and voltage error caused by series resistance as described in the Materials and Methods. (*a*) This cell expressed a combination of rapidly and slowly inactivating current. Currents were elicited by voltage steps to +50 mV from holding potentials (HP) of −120 mV or −70 mV as indicated in the figure. Fitting the function

$$A_f \times e^{-t/\tau_f} + A_s \times e^{-t/\tau_s} + C$$

to the current decay gave τ_f = 4.42 ms and τ_s = 210 ms inactivation time constants for the rapid and slow components, respectively, and a ratio of A_s to A_f of 0.065. The current elicited by a step to + 50 mV from −70 mV holding potential could be well-fit with a single-exponential function with a time constant of τ_{inact} = 186.5 ms. Sampling frequency, cell capacitance and series resistance were 1 kHz, 3.5 pF and 8.3 MΩ, respectively. The *R* values are 0.002 and 0.028 for holding potentials of −120 and −70 mV, respectively. (*b*) This cell expressed slowly inactivating current only. Currents were elicited by voltage steps to +50 mV from HP of −120 mV or −70 mV as indicated in the figure. Currents elicited from both holding potentials were well-fit by a single-exponential function with a time constant of τ_{inact} = 142 ms (HP = −120 mV) and τ_{inact} = 154 ms (HP = −70 mV). Sampling frequency, cell capacitance, and series resistance were 666 Hz, 6.6 pF, and 6.8 MΩ, respectively. The *R* values are 0.06 for both holding potentials of −120 and −70 mV.

shown in *b* the fraction of mutant subunits is 0.5. Regardless of the value of *p*, the function derived from a binomial distribution gives excellent fits to the data. However, very poor fits were obtained for traces where the current inactivation had a clearly biphasic character, as can be seen in Fig. 3 *c*. Fitting a sum of two exponential functions to the trace resulted in a fast component with τ_f = 7.7 ms (> τ_4) and a slow component with τ_0 = 194 ms, indicating the presence of heterotetrameric channels responsible for the fast component of the decay. Because Jurkat cells constitutively express endogenous K^+ channels at variable levels (see above), these channels may already be present in the plasma membrane when newly formed homo- and heterotetrameric channels are inserted into the plasma membrane. If the portion of these "preformed" channels is significant, then a slow inactivation phase will be observed. We have modified Eq. 1 to include a term due to the presence of preformed WT channels:

$$\frac{I(t)}{I_{peak}} = (1 - A)\sum_{m=0}^{4} B_{4,m}\left((1 - R)\,e^{-\frac{t}{\tau_m}} + R\right) + A\left((1 - R)\,e^{-\frac{t}{\tau_0}} + R\right), \quad (3)$$

where *A* represents the fraction of preformed channels. Fitting Eq. 3 to the inactivating phase of current traces *c* and *d* in Fig. 3 gave excellent fits, regardless of the value of *A*. For approximately the same distribution of homo- and heterotetrameric channels (*p* = 0.84 and 0.79 for *c* and *d*, respectively), the fraction of preformed channels was 0.22 and 0.10, respectively. The fractions of preformed channels for the cells shown in Fig. 3, *a* and *b* were essentially 0. Using Eq. 3, we have successfully fit heterotetrameric currents for 26 cells. The *p* values range from 0.19 to 0.88 and the *A* values range from 0 to 0.5. The values of *p* and *A* are highly reproducible within a single cell. Duplicate pulses to +50 mV, separated by 3 min, gave currents that could be fit with *p* and *A* values that differed by 0.007 ± 0.011 and 0.006 ± 0.006 (± SEM, *n* = 15), respectively.

Distribution of Channel Subtypes

As demonstrated in Figs. 1 and 3, cells transfected with the A413V channel gene express a diversity of currents, which as shown above, can be statistically analyzed to identify the subpopulations of homo- and heterotetrameric channels. The distribution of these subpopulations is determined mainly by the relative concentration of A413V and WT subunits, which are, in turn, influenced by the initial DNA concentration used to transfect the cells, the relative kinetics and magnitude of subunit formation, degradation rates and the time after transfection. These factors most likely account for

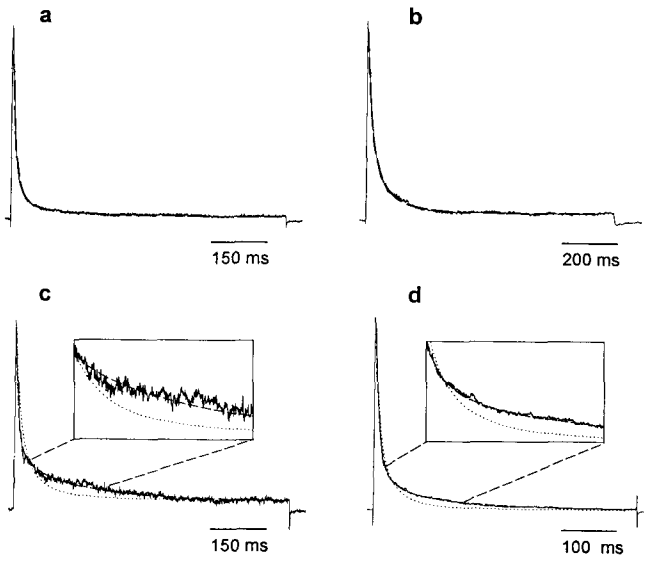

FIGURE 3. Whole-cell currents from Jurkat Tag C15 cells expressing mixtures of WT/A413V homo- and heterotetramers. In *a–d* four different cells were transfected with Kv1.3(A413V)/CD20 double-gene plasmid (25 nM) and patch-clamped 24–72 h later. Currents were elicited by a voltage step to +50 mV from the holding potential of −120 mV. The current traces were corrected for ohmic leak and voltage error caused by series resistance as described in the Materials and Methods, and were normalized to their respective peak (——). The decaying part of the currents was fit using Eq. 3. (*a*) This cell has a capacitance of 10 pF, series resistance of 5.6 MΩ, peak current of 848 pA and the sampling frequency was 2.66 kHz. Eq. 3 gave an excellent fit to the data (– – –·) with $p = 0.8$ and $A = 0.03$; and the sum of squared errors was (SSE) 0.1. Differences in p and A values determined from duplicate pulses were −0.05 and −0.01, respectively. (*b*) This cell has a capacitance of 12 pF, series resistance of 11 MΩ and peak current of 742 pA. The sampling frequency was 1 kHz. Eq. 3 gave an excellent fit to the data (– – –·) with $p = 0.50$, $A = 0$, and the SSE was 0.06. When $A = 0$, Eq. 3 equals Eq. 1; therefore in *a* and *b* the dashed lines represent both the fits of Eq. 1. or Eq. 3 to the data. Differences in p and A values determined from duplicate pulses were −0.05 and 0, respectively. (c) This cell has a capacitance of 4.7 pF, series resistance of 16 MΩ and peak current of 345 pA. The sampling frequency was 2.66 kHz. Eq. 3 gave an excellent fit to the data (– – –·) with $p = 0.84$, $A = 0.22$, and the SSE was 0.4. If $A = 0$, then Eq. 3 becomes Eq. 1 and gives a poor fit (. . . . . .) with $p = 0.57$ and the SSE was 2.76. Differences in p and A values determined from duplicate pulses were 0.01 and 0.01, respectively. (*d*) This cell has a capacitance of 4.4 pF, series resistance of 3.3 MΩ and peak current of 1445 pA. The sampling frequency was 3.9 kHz. Eq. 3 gave an excellent fit to the data (– – –·) with $p = 0.79$, $A = 0.1$, and the SSE was 0.09. If $A = 0$, then Eq. 3 becomes Eq. 1 and gives a poor fit (. . . . . .) with $p = 0.67$ and the SSE was 1.06. Differences in p and A values determined from duplicate pulses were 0.06 and 0.02, respectively. The insets in *c* and *d* show the indicated segments of the current traces and fits enlarged by 2.2-fold. R values were 0.015, 0.04, 0.054, and 0.002 for *a–d*, respectively.

the diversity of currents in Fig. 1. Calculations from the binomial distribution indicate that heterotetrameric channels dominate the channel distribution if the fraction of a mutant subunit in the membrane, p, is between 0.84 (i.e., fraction of A413V homotetrameric channels is $p^4 \leq 0.49$) and 0.16 (i.e., fraction of WT homotetrameric channels is $(1-p)^4 \leq 0.49$). Excessive production of either WT ($p < 0.16$) or A413V ($p > 0.84$) will lead to a predominance of homotetramers. Jurkat Tag C15 cells express constitutively low levels of endogenous WT channels (see above); therefore the level of expression of A413V subunits will determine not only the amplitude of the measured current but also the distribution of channel subtypes. Cells expressing predominantly heterotetrameric channels should have current amplitudes intermediate between cells expressing only WT and cells expressing only A413V homotetramers. Cells expressing more heterologous subunits will display more current and the distribution of peak current amplitudes should be shifted toward that obtained for cells expressing predominantly A413V homotetramers.

To examine the relationship of peak current amplitudes to the distribution of channel subpopulations, we compared the current amplitude at +50 mV for cells classified as expressing predominantly WT, A413V or heterotetrameric currents as described in the Materials and Methods section. Fig. 4 shows the amplitude histogram of the peak current at +50 mV for cells expressing predominantly heterotetrameric current (median = 742 pA, 25 and 75 percentiles are 424 pA and 1000 pA, respectively, $n = 31$) along with the vertical lines indicating the medians of the peak currents for cells expressing either predominantly WT homotetramers (median = 479 pA, 25 and 75 percentiles are 325 pA and 600 pA, respectively, $n = 23$), predominantly heterotetramers, or predominantly A413V current (median = 2927 pA, 25 and 75 percentiles are 1162 pA and 6190 pA, respectively, $n = 37$). The distributions of the peak currents were significantly different amongst the three categories ($P < 0.0001$, Kruskal-Wallis ANOVA on ranks).

The dependence of the formation of heterotetrameric channels on the A413V subunit concentration was directly assessed by transfecting cells with A413V Kv1.3 at two different plasmid concentrations. We sampled 37 and 40 cells, respectively, for 25 and 8 nM A413V DNA concentration, between 6 and 18 h after transfection. The distributions showed that 1, 22, and 14 cells expressed predominantly WT homotetramers, A413V homotetramers and heterotetramers, respectively, for the higher concentration, and 1, 10, and 29 cells, respectively, for the lower concentration. A 3 × 2 (contingency) Chi Square test gave $P < 0.01$, indicating that at high levels of A413V DNA, homotetrameric

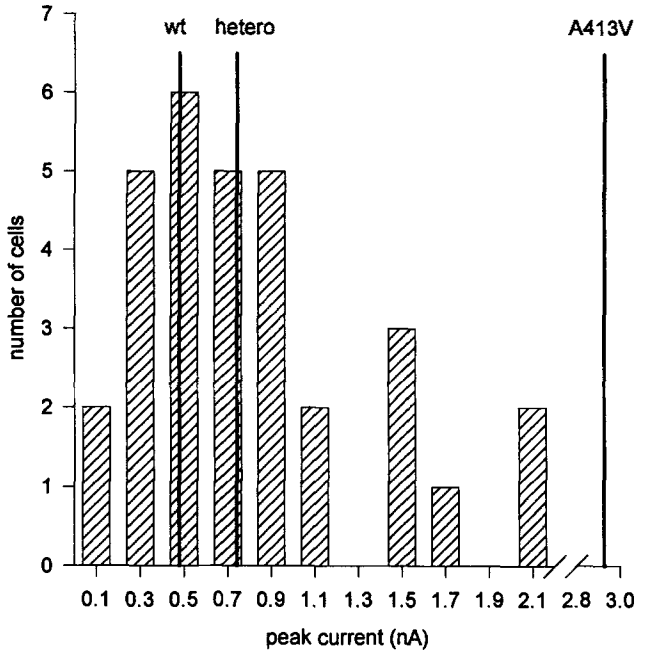

FIGURE 4. Distribution of the peak currents in cells expressing heterotetrameric currents. Cells were transfected with Kv1.3 (A413V)/CD20 double-gene plasmid (25 nM) and patch-clamped 24–72 h later. Currents were elicited by a voltage step to +50 mV from the holding potential of −120 mV and the peak currents were measured after correcting for ohmic leak and voltage error caused by series resistance as described in the Materials and Methods. The frequency histogram was created from the peak currents in cells expressing predominantly heterotetrameric currents (n = 31) using a class interval of 0.2 nA. The vertical lines indicate the median of the peak currents in cells expressing predominantly homotetrameric WT (479 pA, n = 23), heterotetrameric (742 pA, n = 31) and homotetrameric A413V currents (2927 pA, n = 37), as indicated. In all pairwise multiple comparisons (Dunn's Method) the peak currents in cells expressing predominantly A413V current were significantly different from those derived from WT or heterotetrameric current expressing cells ($P < 0.05$).

A413V channels predominate, whereas at low A413V DNA levels, heterotetrameric channels predominate. There is a significant difference ($P < 0.016$, Mann-Whitney Rank Sum test) between the peak currents at +50 mV measured in cells transfected at 8 nM (median = 1120 pA) and those measured in cells transfected with 25 nM (median = 1570 pA) of A413V/CD20 plasmid DNA.

Suppression of the Endogenous Current

Efficient expression of heterotetrameric current derived from endogenous WT and heterologous mutant A413V Kv1.3 is achieved in Jurkat (~35% of the cells) using a plasmid concentration of 25 nM. These heterotetramers are formed as early as 6 h after the transfection. We have used this information to carry out suppression of endogenous Kv1.3 channels in Jurkat cells. We, and others, have shown previously that truncated NH_2-terminal segments of voltage-gated K^+ channels can specifically suppress the heterologous expression of the corresponding full-length K^+ channel (Li et al., 1992; Babila et al., 1994; Tu et al., 1995). In CTLL-2, a truncated sequence containing the first 866 bases of the translated portion of the Kv1.3 gene (Kv1.3 (+866)) completely suppresses the heterologously expressed Kv1.3 K^+ current (Tu et al., 1995). If the mechanism of suppression involves formation of heterotetramers composed of full-length subunits and truncated channel fragments, then by analogy to the experiments producing endogenous+heterologous hybrid channels, a high concentration of truncated channel DNA must be used in the transfection, and the time of assay for suppression should be appropriate for the kinetics of expression of truncated subunits. The critical determinant for suppression is concomitant degradation of preformed WT channels and formation of heterotetrameric channels. This condition is met within the first 18 h after transfection, as reported in the previous section.

Suppression was evaluated by comparing peak currents recorded from Jurkat cells transfected with 25 nM of the double-gene plasmid (pRc/CMV/Kv1.3(+866)/mCD4, experimental) to peak currents recorded from cells transfected with 25 nM of mCD4 only (control).

Fig. 5 shows the amplitude histogram (*a* and *b*) and the normalized cumulative amplitude distribution (*c* and *d*) of the peak currents at +50 mV for experimental and control samples at 48 h and 72 h after transfection. The difference between the median of the peak current for control and Kv1.3(+866)-transfected cells was significant at 48 h after transfection ($P < 0.001$, Mann-Whitney rank sum test). The median of the peak current was 375 pA (n = 33) for control and 150.7 pA (n = 36) for cells transfected with Kv1.3(+866) at 48 h. The difference was not significant at 72 h after transfection, where the median of the peak current was 323.5 pA (n = 34) for control and 271.5 pA (n = 38) for cells transfected with Kv1.3(+866). These results indicate that the distribution of the peak current is shifted to lower current amplitudes in cells transfected with Kv1.3(+866).

DISCUSSION

The spatial and temporal domains in which assembly of channels occur will ultimately determine the ability of endogenous subunits to interact with heterologous channel peptides. For instance, if endogenous subunits are processed in segregated compartments or at different times from heterologous peptides, then inter-subunit interactions required for suppression or heterotetramer formation will not occur. In this paper, we show that endogenous Kv1.3 subunits in Jurkat cells can

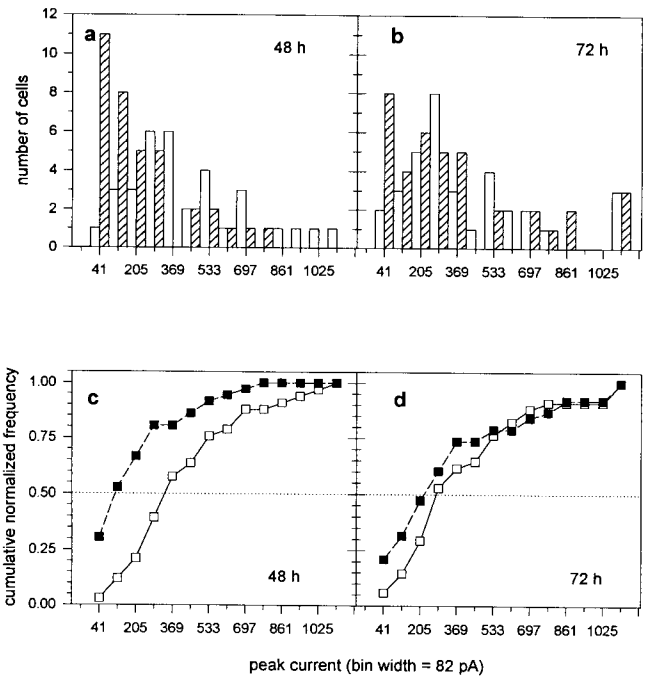

FIGURE 5. Suppression of endogenous Kv1.3 by truncated Kv1.3 (+866) in Jurkat Tag C15 cells. Cells were transfected with Kv1.3(+866)/mCD4 double-gene plasmid (25 nM) or with mCD4 (25 nM). The peak current elicited by a voltage step to +50 mV from the holding potential of −80 mV was measured 48 and 72 h after the transfection. (*a* and *b*) The histograms show the distribution of the peak currents in cells transfected with the truncated K^+ channel DNA (Kv1.3(+866)/mCD4, shaded bars) and in control cells transfected with mouse CD4 (empty bars) at 48 (*a*) and 72 h (*b*) after the transfection. (*c* and *d*) The cumulative normalized distributions of the peak currents shown in *c* and *d* were constructed from *a* and *b*, respectively. Symbols ■ and □ indicate the distributions for cells transfected with Kv1.3(+866)/mCD4 and mCD4 (control), respectively. The dotted line indicates 50% of the data (median).

form heterotetramers with heterologously transfected mutant Kv1.3 subunits, indicating that synthesis and assembly of subunits occur concomitantly in shared compartments.

Although the exact compartments that are shared by non-identical monomeric subunits were not directly assayed, we can deduce some characteristics of K^+ channel assembly from our experimental results. Table I indicates the distribution of channel types predicted by the models for assembly of two different subunits (e.g., WT and A413V; open and closed circles, respectively) based on general features of whether (*a*) WT and A413V pools are segregated vs. integrated, (*b*) tetramerization is an equilibrium vs. irreversible process, and (*c*) irreversibly formed tetramers exist in the plasma membrane. In case I, WT and A413V pools are segregated and result in a bimodal distribution of channels. The inactivation kinetics for such a distribution of channels will be well-described by a function with two exponential terms, each containing the inactivation time constant for WT and A413V homotetramer. Segregation can be either spatial or temporal. However, our data show that if segregation (bimodality) occurs (e.g., Fig. 1 *e*), it must be temporal because heterotetramers are also formed in the same transfected cell population. In case II an integrated monomeric pool is in equilibrium with heterotetramers. This predicted distribution of channel species is binomial, regardless of the presence or absence of preformed WT homotetramers. The inactivation kinetics will therefore be described by Eq. 1. In cases III and IV tetramers are irreversibly formed from an integrated pool of monomers. If no preformed WT channels are present, then the predicted distribution will be binomial (case III); if preformed WT channels are present, then the distribution will be binomial plus a constant (case IV). The inactivation kinetics for case IV will be described by Eq. 3. Although experimental conditions can be created that conform to cases I-III (e.g., Fig. 1, *a–e* and 3, *a–b*), a channel distribution that is binomial plus a constant will occur only if case IV is true.

Our findings (see Fig. 3) are consistent with case IV and permit the following conclusions to be made regarding K^+ channel assembly. First, subunits are recruited randomly from integrated monomer pools. Therefore, we can infer that Kv1.3 monomers diffuse individually in the ER membrane before oligomerizing and that the four subunits in any given tetramer were not translated and preferentially assembled from the same polysome. These conclusions are similar to those made for mixed trimer formation of influenza virus hemagglutinin (Boulay et al., 1988) and may be true for many oligomeric transmembrane proteins. The second conclusion from our results is that tetramers formed from integrated monomer pools are found in the plasma membrane and do not dissociate on a timescale of 6–72 h. This is in contrast to the voltage-gated sodium channel, which is composed of one large, heavily glycosylated α subunit and one or two smaller β subunits (Hartshorne and Catterall, 1981; Hartshorne et al., 1982; Hartshorne and Catterall, 1984; Roberts and Barchi, 1987). One of the β subunits is noncovalently associated with the α subunit, and oligomerization of heterologously expressed α and β subunits can occur in the plasma membrane of *Xenopus* oocytes (Agnew, W., personal communication). These findings, however, may reflect differential processing of some proteins (Ukomadu et al., 1992) in different expression systems. For example, when the Na^+,K^+-ATPase α and β subunits are expressed in *Xenopus* oocytes, protein accumulates in the ER until oligomerization is complete (Geering et al., 1989; Ackerman and Geer-

TABLE I

Models for Assembly and Distribution of Tetrameric K^+ Channels

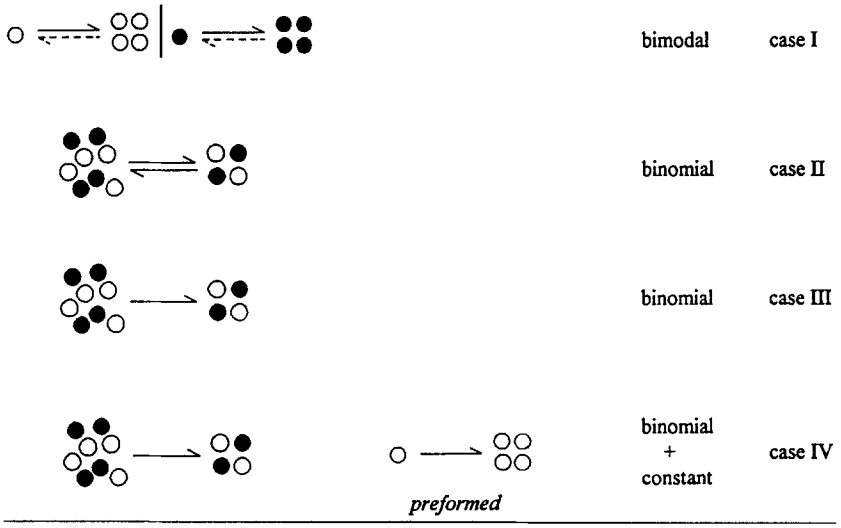

The symbols ○ and ● represent the monomeric Kv1.3 WT and A413V subunits, respectively. The vertical line separating the WT and A413V subunits in the segregated model indicates there is a barrier between subunit pools. Tetrameric channels are represented as a symmetric arrangement of four symbols, while random mixture of eight symbols indicates a pool of mixed monomeric subunits. The dashed backward arrows indicate that an equilibrium may exist.

ing, 1990; Jaunin et al., 1992). However, in Sf-9 insect cells, α and β subunits expressed separately translocate to the plasma membrane, and if cells containing only one subunit fuse with cells containing the other subunit, the different subunits will mix to form functional Na^+, K^+-ATPases (DeTomaso et al., 1994). The lack of dissociation of K^+ channel tetramers in the plasma membrane is similar to what is observed for most membrane oligomers (Hurtley and Helenius, 1989). However, dissociation and reassociation of oligomeric protein subunits can occur in the ER. For example, vesicular stomatitis virus glycoprotein, a noncovalently linked trimer is in equilibrium with monomers in the ER (Zagouras et al., 1991).

Both the extent and kinetics of heterotetramer formation and suppression of endogenous Kv1.3 depend on the relative production of endogenous vs. heterologous subunits at any given time. This, in turn, is dependent on the corresponding synthesis and degradation rates of endogenous WT Kv1.3 and of heterologous gene products. These rates may be influenced by cell cycle. Evidence that Kv1.3 channel number can be up- and down-regulated with cell cycle progression has been demonstrated at the plasma membrane level (Deutsch et al., 1986; Lee et al., 1986; Decoursey et al., 1987) and at the mRNA level (Cai et al., 1992; although, see Price et al., 1993). Endogenous and heterologous Kv1.3 genes are differentially regulated under different promoter control, with transcription of the heterologous genes regulated by a CMV promoter. In mammalian cells, vis-a-vis oocytes, it is possible to study the mechanisms by which the relative kinetics of endogenous and heterologous expression are regulated to effect heterotetramerization and/or suppression, especially since some of these mechanisms may be a function of cell cycle.

Even within the same lymphoid expression system, there may be different factors that will determine kinetics for heterotetramer formation and suppression of endogenous channels. We have observed that heterotetramer formation and suppression may occur with dissimilar kinetics (data not shown). The heterologous Kv1.3 gene used in each case is different: in heterotetramer formation experiments, the heterologous gene is a full-length A413V mutant Kv1.3, whereas in suppression experiments, the heterologous gene is a truncated Kv1.3. Other considerations include relative rate constants for tetramer formation and stability of tetramer vs. monomer-truncated complexes, cell cycle, concentrations of monomer A413V vs. truncated Kv1.3. Moreover, synthesis and degradation of truncated Kv1.3, which may be recognized as incorrectly folded, may be much faster than synthesis and degradation of the full-length A413V monomer.

We show here that constitutively expressed endogenous Kv1.3 channels can be suppressed by truncated Kv1.3 peptides. Previously we showed that up-regulated endogenous *Shaker*-like currents in GH3 cells (an anterior pituitary cell line) can be suppressed (Tu et al., 1995). In both GH3 and Jurkat cells, however, constitu-

tively expressed K^+ channels could not be suppressed by truncated Kv1.3. Three reasons for the previous failure to observe suppression in Jurkat are that (*a*) the sampling size for control and experimental groups was too small, (*b*) the concentration of plasmid was too low, and (*c*) the time at which suppression was assayed by electrophysiological recording was too late after transfection and at a time when truncated peptide concentration was too low to cause suppression.

Our findings have implications for the regulation of diversity of K^+ channel expression in mammalian cells. The amount of mixing of subunit pools within subfamilies depends on the respective kinetics of expression. Different monomers will remain as separate, segregated pools if subunit synthesis of the different isoforms is separated in time. To keep two isoforms of the same subfamily separate, for example, during selective up-regulation of one isoform vs. another (e.g., as occurs with hormone stimulation of pituitary and cardiac cells [Attardi et al., 1993; Takimoto et al., 1995; Takimoto and Levitan, 1994]) the cell cannot use separate spatial compartments. It must adjust the relative times and rates of subunit expression. On the other hand, heterotetrameric channels of the *Shaker* subfamily have been detected in mammalian neurons in vivo (Wang et al., 1993; Sheng et al., 1993). These channels must assemble from concurrently translated subunits. Since the heterotetramers are only a fraction of the K^+ channels in these cells, translation need only overlap temporally for a short time. The degree of temporal overlap will determine the proportion of hetero- and homotetramers.

We thank LiWei Tu and ZuFang Sheng for constructing the pRc/CMV/A413V/CD20, pRc/CMV/Kv1.3(+866)/mCD4, and pRc/CMV/mCD4 plasmids. We thank Richard Horn, Robert Doms, and Daniel Levy for their critical reading of the manuscript.

This work was supported by National Institutes of Health Grant GM 52302 and Grant No. FO5 TWO 5079 from the Fogarty International Center (FIC), National Institutes of Health (NIH). The contents of the publication are solely the responsibility of the authors and do not necessarily represent the official views of the FIC, NIH.

Received for publication 2 November 1995 and accepted version received 8 December 1995.

REFERENCES

Ackermann, U., and K. Geering. 1990. Mutual dependence of Na, K-ATPase α- and β-subunit for correct posttranslational processing and intracellular transport. *FEBS Lett.* 269:105–108.

Attardi, B., K. Takimoto, R. Gealy, C. Severns, and E.S. Levitan. 1993. Glucocorticoid induced up-regulation of a pituitary K^+ channel mRNA *in vitro* and *in vivo*. *Recept. Channels.* 1:287–293.

Babila, T., A. Moscucci, H. Wang, F.E. Weaver, and G. Koren. 1994. Assembly of mammalian voltage-gated potassium channels: evidence for an important role of the first transmembrane segment. *Neuron.* 12:615–626.

Bono, M.R., V. Simon, and M.S. Rosemblatt. 1989. Blocking of human T lymphocyte activation by channel antagonists. *Cell Biochem. Funct.* 7:219–226.

Boulay, F., R.W. Doms, R.G. Webster, and A. Helenius. 1988. Posttranslational oligomerization and cooperative acid activation of mixed influenza hemagglutinin trimers. *J. Cell Biol.* 106:629–639.

Cahalan, M.D., K.G. Chandy, T.E. Decoursey, and S. Gupta. 1985. A voltage-gated potassium channel in human T lymphocytes. *J. Physiol. (Lond.).* 358:197–237.

Cai, Y.C., P.B. Osborne, R.A. North, D.C. Dooley, and J. Douglass. 1992. Characterization and functional expression of genomic DNA encoding the human lymphocyte type *n* potassium channel. *DNA Cell Biol.* 11:163–172.

Carlin, B.E., and J.P. Merlie. 1986. Assembly of multisubunit membrane proteins. *In* Protein Compartmentalization. A.W. Strauss, I. Boime, and G. Kreil, editors. Springer-Verlag, NY. 71–86.

Decoursey, T.E., K.G. Chandy, S. Gupta, and M.D. Cahalan. 1985. Voltage-dependent ion channels in T-lymphocytes. *J. Neuroimmunol.* 10:71–95.

Decoursey, T.E., K.G. Chandy, S. Gupta, and M.D. Cahalan. 1987. Mitogen induction of ion channels in murine T lymphocytes. *J. Gen. Physiol.* 89:405–420.

DeTomaso, A.W., G. Blanco, and R.W. Mercer. 1994. The α and β subunits of the Na,K-ATPase can assemble at the plasma membrane into functional enzyme. *J. Cell Biol.* 127:55–69.

Deutsch, C., and L. Chen. 1993. Heterologous expression of specific K^+ channels in T lymphocytes: functional consequences for volume regulation. *Proc. Natl. Acad. Sci. USA.* 90:10036–10040.

Deutsch, C., A. Holian, S.K. Holian, R.P. Daniele, and D.F. Wilson. 1979. Transmembrane electrical and pH gradients across human erythrocytes and human peripheral lymphocytes. *J. Cell. Physiol.* 99:79–93.

Deutsch, C., D. Krause, and S.C. Lee. 1986. Voltage-gated potassium conductance in human T lymphocytes stimulated with phorbol ester. *J. Physiol. (Lond.).* 372:405–423.

Deutsch, C., M. Price, S. Lee, V.F. King, and M.L. Garcia. 1991. Characterization of high affinity binding sites for charybdotoxin in human T lymphocytes. Evidence for association with the voltage-gated K^+ channel. *J. Biol. Chem.* 266:3668–3674.

Doms, R.W., R.A. Lamb, J.K. Rose, and A. Helenius. 1993. Folding and assembly of viral membrane proteins. *Virology.* 193:545–562.

Efron, B., and R. Tibshirani. 1984. Bootstrap methods for standard errors, confidence intervals, and other measures of statistical accuracy. *Statistical Sci.* 1:54–77.

Freedman, B.D., M. Price, and C. Deutsch. 1992. Evidence for voltage modulation of IL2 production by human blood lymphocytes. *J. Immunol.* 149:3784–3794.

Geering, K., I. Theulaz, F. Verrey, M.T. Hauptle, and B.C. Rossier. 1989. A role for the β-subunit in the expression of functional Na,K-ATPase in *Xenopus* oocytes. *Am. J. Physiol.* 257:C851–C858.

Gelfand, E.W., R.K. Cheung, and S. Grinstein. 1984. Role of membrane potential in the regulation of lectin-induced calcium uptake. *J. Cell. Physiol.* 121:533–539.

Grinstein, S., and J.D. Smith. 1990. Calcium-independent cell volume regulation in human T lymphocytes. Inhibition by charybdotoxin. *J. Gen. Physiol.* 95:97–120.

Hartshorne, R.P., and W.A. Catterall. 1981. Purification of the saxitoxin receptor of the sodium channel from rat brain. *Proc. Natl. Acad. Sci. USA.* 78:4620–4624.

Hartshorne, R.P., and W.A. Catterall. 1984. The sodium channel from rat brain. Purification and subunit composition. *J. Biol. Chem.* 259:1667–1675.

Hartshorne, R.P., D.J. Messner, J.C. Coppersmith, and W.A. Catterall. 1982. The saxitoxin receptor of the sodium channel from rat brain. Evidence for two nonidentical beta subunits. *J. Biol. Chem.* 257:13888–13891.

Hopkins, W.F., V. Demas, and B.L. Tempel. 1994. Both N- and C-terminal regions contribute to the assembly and functional expression of homo- and heteromultimeric voltage-gated K^+ channels. *J. Neurosci.* 14:1385–1393.

Hurtley, S.M., and A. Helenius. 1989. Protein oligomerization in the endoplasmic reticulum. *Ann. Rev. Cell Biol.* 5:277–307.

Jaunin, P., J.-D. Horisberger, K. Richter, P.J. Good, B.C. Rossier, and K. Geering. 1992. Processing, intracellular transport, and functional expression of endogenous and exogenous α-β Na,K-ATPase complexes in Xenopus oocytes. *J. Biol. Chem.* 267:577–585.

Lee, S.C., D.I. Levy, and C. Deutsch. 1992. Diverse K^+ channels in primary human T lymphocytes. *J. Gen. Physiol.* 99:771–793.

Lee, S.C., D.E. Sabath, C. Deutsch, and M.B. Prystowsky. 1986. Increased voltage-gated potassium conductance during interleukin 2-stimulated proliferation of a mouse helper T lymphocyte clone. *J. Cell Biol.* 102:1200–1208.

Lee, T.E., L.H. Phillipson, A. Kuznetsov, and D.J. Nelson. 1994. Structural determinant for assembly of mammalian K^+ channels. *Biophys. J.* 66:667–673.

Leonard, R., M.L. Garcia, R.S. Slaughter, and J.P. Reuben. 1992. Selective blockers of voltage-gated K^+ channels depolarize human T lymphocytes: mechanism of the antiproliferative effect of charybdotoxin. *Proc. Natl. Acad. Sci. USA.* 89:10094–10098.

Li, M., Y.N. Jan, and L.Y. Jan. 1992. Specification of subunit assembly by the hydrophilic amino-terminal domain of the Shaker potassium channels. *Science (Wash. DC).* 257:1225–1230.

Lin, C.S., R.C. Boltz, J.T. Blake, M. Nguyen, A. Talento, P.A. Fischer, M.S. Springer, N.H. Sigal, R.S. Slaughter, M.L. Garcia et al. 1993. Voltage-gated potassium channels regulate calcium-dependent pathways involved in human T lymphocyte activation. *J. Exp. Med.* 177:637–645.

MacKinnon, R. 1991. Determination of the subunit stoichiometry of a voltage-activated potassium channel. *Nature (Lond.).* 350:232–235.

Matteson, D.R., and C. Deutsch. 1984. K^+ channels in T lymphocytes: a patch clamp study using monoclonal antibody adhesion. *Nature (Lond.).* 307:468–471.

Northrop, J.P., K.S. Ullman, and G.R. Crabtree. 1993. Characterization of the nuclear and cytoplasmic components of the lymphoid-specific nuclear factor of activated T cells (NF-AT) complex. *J. Biol. Chem.* 268:2917–2923.

Panyi, G., Z. Sheng, L.-W. Tu, and C. Deutsch. 1995. C-type inactivation of a voltage-gated K^+ channel occurs by a cooperative mechanism. *Biophys. J.* 69:896–904.

Price, M., B.D. Freedman, R.A. Swanson, K. Folander, and C. Deutsch. 1993. Modulation of K^+ channel mRNA in primary human T lymphocytes. *Biophys. J.* 67:A197 (Abstr.).

Rink, T.J., C. Montecucco, T.R. Hesketh, and R.Y. Tsien. 1980. Lymphocyte membrane potential assessed with fluorescent probes. *Biochim. Biophys. Acta.* 595:15–30.

Roberts, R.H., and R.L. Barchi. 1987. The voltage-sensitive sodium channel from rabbit skeletal muscle. *J. Biol. Chem.* 262:2298–2303.

Rotundo, R.L. 1984. Asymmetric acetylcholinesterase is assembled in the Golgi apparatus. *Proc. Natl. Acad. Sci. USA.* 81:479–483.

Santacruz-Toloza, L., Y. Huang, S.A. John, and D.M. Papazian. 1994. Glycosylation of *Shaker* potassium channel protein in insect cell culture and in *Xenopus* oocytes. *Biochemistry.* 33:5607–5613.

Shen, N.V., X. Chen, M.M. Boyer, and P. Pfaffinger. 1993. Deletion analysis of K^+ channel assembly. *Neuron.* 11:67–76.

Shen, N.V. and P.J. Pfaffinger. 1995. Molecular recognition and assembly sequences involved in the subfamily-specific assembly of voltage-gated K^+ channel subunit proteins. *Neuron.* 14:625–633.

Sheng, M., Y.L. Liao, Y.N. Jan, and L.Y. Jan. 1993. Presynaptic A-current based on heteromultimeric K^+ channels detected *in vivo. Nature (Lond.).* 365:72–75.

Sporn, L.A., V.J. Marder, and D.D. Wagner. 1986. Inducible secretion of large, biologically potent von Willebrand factor multimers. *Cell.* 46:185–190.

Takimoto, K., R. Gealy, A.F. Fomina, J.S. Trimmer, and E.S. Levitan. 1995. Inhibition of voltage-gated K^+ channel gene expression by the neuropeptide thyrotropin-releasing hormone. *J. Neurosci.* 15:449–457.

Takimoto, K., and E.S. Levitan. 1994. Glucocorticoid induction of Kv1.5 K^+ channel gene expression in ventricle of rat heart. *Circ. Res.* 75:1006–1013.

Tu, L.-W., V. Santarelli, and C. Deutsch. 1995. Truncated K^+ channel DNA sequences specifically suppress lymphocyte K^+ channel gene expression. *Biophys. J.* 68:147–156.

Ukomadu, C., J. Zhou, F.J. Sigworth, and W.S. Agnew. 1992. μI Na^+ channels expressed transiently in human embryonic kidney cells: biochemical and biophysical properties. *Neuron.* 8:663–676.

Wang, H., D.D. Kunkel, T.M. Martin, P.A. Schwartzkroin, and B.L. Tempel. 1993. Heteromultimeric K^+ channels in terminal and juxtaparanodal regions of neurons. *Nature (Lond.).* 365:75–79.

Zagouras, P., A. Ruusala, and J.K. Rose. 1991. Dissociation and reassociation of oligomeric viral glycoprotein subunits in the endoplasmic reticulum. *J. Virol.* 65:1976–1984.